

Theory of phase-locking in small Josephson junction cells

M. Basler*, W. Krech† and K. Yu. Platov‡

Friedrich-Schiller-Universitt Jena

Institut fr Festkrperphysik

07743 Jena

Max-Wien-Platz 1

(February 13, 1995)

Abstract

Within the RSJ model, we performed a theoretical analysis of phase-locking in elementary strongly coupled Josephson junction cells. For this purpose, we developed a systematic method allowing the investigation of phase-locking in cells with small but non-vanishing loop inductance. The voltages across the junctions are found to be locked with very small phase difference for almost all values of external flux. However, the general behavior of phase-locking is found to be just contrary to that according to weak coupling. In case of strong coupling there is nearly no influence of external magnetic flux on the phases, but the locking-frequency becomes flux-dependent. The influence of parameter splitting is considered as well as the effect of small capacitive shunting of the junctions. Strongly coupled cells show synchronization even for large parameter splitting. Finally, a study of the behavior under external microwave radiation shows that the frequency locking-range becomes strongly

*pmb@rz.uni-jena.de

†owk@rz.uni-jena.de

‡okp@rz.uni-jena.de

flux-dependent, whereas the locking frequency itself turns out to be flux-independent.

74.50

I. INTRODUCTION

Josephson junction arrays are considered as candidates for microwave oscillators with possible applications in the field of satellite communication systems, astronomical observations, construction of supercomputer chips and spectroscopy¹⁻⁹. They are potentially well tunable over a relatively wide frequency range while radiating on a narrow linewidth, and they can deliver large output power, at least in comparison with a single element. Linear arrays of Josephson junctions have been subject to theoretical investigation for more than twenty years^{1,3,8,10-12}. During last years, there have been some promising experimental results¹³⁻¹⁵. Since the beginning of the nineties, there has been a growing interest in 2D arrays^{4,5,16-21}. Up to now, the radiation power of 2D arrays was found to be much smaller than that of 1D arrays ($0,1 \mu\text{W}$ maximum¹⁸, in comparison to $50 \mu\text{W}$ in 1D arrays¹⁵). This may be a consequence of technological problems as well as of general properties of 2D arrays.

Because of this fact, there is some renewed interest in the general mechanisms of synchronization of coupled Josephson junctions. Most of the early adiabatic investigations were based on weak (preferably inductive) coupling of the elements^{1,22-28}, which is surely fulfilled for relatively large circuits with total inductances $\gtrsim 10$ pH. However, present day technology allows the preparation of very compact arrays with circuit dimensions around $1 \mu\text{m}$ and smaller, having inductances smaller than 3pH. In this case, the adiabatic methods developed earlier fail. On the other hand, neglecting inductances at all²⁹ seems to be a too rough approximation.

In this paper we develop a method for dealing with Josephson junctions coupled via a small inductive shunt (SQUID-type coupling) in a systematic way. In Sec. II, we describe the circuits handled by this method, derive the general equations, review some results obtained by conventional methods and discuss their inapplicability to our problem. In Sec. III, we give a review of our analytical method and present some results for the simplest case of non-hysteretical, identical junctions, which are compared with numerical simulations. Sec. IV is devoted to non-identical junctions and Sec. V to the influence of an additional small junction

capacitance. In Sec. VI we consider the synchronization of strongly coupled SQUID cells by external microwave radiation. A summary as well as some speculations about possible applications of our results are given in Sec. VII.

Contrary to most theoretical investigations which are mainly based on computer simulations during the last years, we concentrate on approximate analytical results. The advantage of this approach is usually a better insight into physical mechanisms in combination with a broader range of applicability concerning the choice of parameters. The disadvantage is a larger amount of mathematical machinery necessary even in relatively simple cases. However, we found it quite valuable to use both methods and compare the results. Some material described in Sec. III was published in a short note earlier³⁰.

II. A SHORT REVIEW ON WEAKLY COUPLED JOSEPHSON JUNCTIONS

The strong coupling method described in this paper was developed for the investigation of the three similar SQUID-like cells shown in Fig. 1, but the general principles should have a much wider range of applicability. These three circuits have a bias current $2I_0$, a net loop inductance L and a parallel biasing scheme in common. Elaborating the equations of motion within the RSJ model, one obtains for the case of identical junctions

$$\dot{\phi}_1 + \sin \phi_1 = i_0 - l^{-1}(\phi_1 - \phi_2 + \varphi), \quad (2.1a)$$

$$\dot{\phi}_2 + \sin \phi_2 = i_0 + l^{-1}(\phi_1 - \phi_2 + \varphi) \quad (2.1b)$$

where ϕ_1 and ϕ_2 are the respective Josephson phases, and i_0 is the normalized bias current,

$$i_0 = I_0/I_C \quad (I_C: \text{critical current}), \quad (2.2)$$

which is supposed to fulfill the condition $i_0 > 1$, here. l marks the normalized loop inductance,

$$l = 2\pi I_C L / \Phi_0, \quad (2.3)$$

and φ the normalized external flux,

$$\varphi = 2\pi\Phi/\Phi_0 \quad (\Phi: \text{external flux, } \Phi_0: \text{flux quantum}). \quad (2.4)$$

Dots denote differentiation w.r.t. the scaled time

$$s = (2e/\hbar)I_C R_N t \quad (R_N: \text{normal resistance}). \quad (2.5)$$

There exist several investigations of these systems for weak coupling, i.e. $l \gg 1^{1,3,26}$. In this case, coupling can be neglected to 0^{th} order w.r.t. l^{-1} and both junctions oscillate with the Josephson phase of an overcritically biased free contact,

$$\phi_{1/2} = \arctan \left[\frac{\zeta_0}{i_0 + 1} \tan \left(\frac{\zeta_0 s - \delta_{1/2}}{2} \right) \right] + \frac{\pi}{2}, \quad (2.6)$$

showing an oscillation frequency

$$\zeta_0 = \sqrt{i_0^2 - 1} \quad (2.7)$$

and constant phases δ_1 and δ_2 . To 1^{st} order the lowest harmonics of solutions (2.6) are inserted into the r.h.s. of Eqs. 2.1a,b. This provides so-called reduced equations for the mean values of the phases, averaged over short time scales of the order of ζ_0 . Looking for solutions of the phase-locking type,

$$\langle \dot{\delta} \rangle = 0, \quad \langle \delta \rangle = \langle \delta_1 \rangle - \langle \delta_2 \rangle, \quad (2.8)$$

one finds

$$\langle \delta \rangle - \frac{1}{i_0(i_0 + \zeta_0)} \sin \langle \delta \rangle = \varphi. \quad (2.9)$$

For usual operation regimes with $i_0 \approx 1.5$ this results in an approximate linear relation between δ and ϕ , as indicated in Fig. 2. The normalized voltages

$$v_{1/2} = \frac{V_{1/2}}{I_C R_N} \quad (2.10)$$

are obtained as

$$v_{1/2} = \frac{\zeta_0^2}{i_0 + \cos(\zeta_0 s - \delta_{1/2})}. \quad (2.11)$$

This procedure and similar adiabatic methods led to a general understanding of the behavior of weakly coupled Josephson junctions. However, they are not applicable to small circuits (of diameter $\lesssim 1\mu\text{m}$) with inductances $\lesssim 1$ pH. The point is, that for small inductances the parameter l^{-1} is not longer small, e.g. $l^{-1} \approx 3$ for $L = 1$ pH and $I_C = 100 \mu\text{A}$. In this case the term in parenthesis on the r.h.s. of Eqs. 2.1a and 2.1b, resp., dominates the remaining terms and it is not possible to derive reduced equations of the type mentioned above.

In order to deal with small inductances which already can be realized technologically today, we developed an alternative systematic scheme, which is described in the next section.

III. A PERTURBATION SCHEME FOR STRONG INDUCTIVE COUPLING

At first, we found it convenient to introduce new variables

$$\Delta = (\phi_2 - \phi_1)/2 \quad \text{and} \quad \Sigma = (\phi_2 + \phi_1)/2, \quad (3.1)$$

providing the set of equations

$$\dot{\Delta} + \cos \Sigma \sin \Delta = \frac{1}{l}(\varphi - 2\Delta), \quad (3.2a)$$

$$\dot{\Sigma} + \sin \Sigma \cos \Delta = i_0. \quad (3.2b)$$

These equations already indicate that the behavior of Σ is determined necessarily by the bias current i_0 and that of Δ by the external flux, although coupling makes things slightly more complicated.

We perform a perturbation expansion valid for small l ,

$$\Delta = \Delta_0 + l\Delta_1 + \mathcal{O}(l^2), \quad (3.3a)$$

$$\Sigma = \Sigma_0 + l\Sigma_1 + \mathcal{O}(l^2). \quad (3.3b)$$

This ansatz resembles the "slowly-varying amplitude method" developed several years ago^{1,31} for l^{-1} then and resulting in reduced equations similar to those mentioned above. Expanding the sin and cos terms, it is not sufficient that the condition

$$|l\Sigma_1| \ll |\Sigma_0| \quad (3.4)$$

is fulfilled, but additionally we must demand the much more rigid conditions

$$|l\Sigma_1| \ll 1 \quad \text{and} \quad |l\Delta_1| \ll 1. \quad (3.5)$$

Investigation of the final result shows, that this can be met for all φ by choosing a sufficiently small l . Only the case $\varphi = \pi$ requires a slightly more involved consideration.

After inserting the expansion (3.3a,b) into Eqs. 3.2a,b one can compare identical powers of l . To lowest, i.e. $(-1)^{st}$, order one finds

$$\Delta_0 = \varphi/2 \quad (3.6)$$

without solving any differential equation. This general feature is valid for higher orders of l , too: The variables Σ_n must be determined by solving a first-order differential equation (only to lowest (0^{th}) order being non-linear), whereas the Δ 's can be calculated algebraically.

Introducing a once more rescaled time,

$$\tilde{s} = s \cdot \cos(\varphi/2), \quad ' = \frac{d}{d\tilde{s}}, \quad (3.7)$$

the equation for Σ_0 (0^{th} order w.r.t. l) becomes very similar to that of an autonomous junction,

$$\Sigma_0' + \sin \Sigma_0 = \tilde{i}_0, \quad \tilde{i}_0 = i_0 / \cos(\varphi/2). \quad (3.8)$$

Thus, we can immediately write down the solution,

$$\Sigma_0 = 2 \arctan \left(\frac{\bar{\zeta}_0}{i_0 + \cos(\varphi/2)} \tan \left(\frac{\bar{\zeta}_0 s}{2} \right) \right) + \frac{\pi}{2}, \quad (3.9)$$

with

$$\bar{\zeta}_0 = \sqrt{i_0^2 - \cos^2(\varphi/2)} \quad (3.10)$$

where we have imposed the initial condition

$$\Sigma_0(s=0) = \pi/2. \quad (3.11)$$

Because the Δ_n are determined algebraically there is no freedom to specify separate initial conditions for them. To ensure the validity of the perturbation expansion, it is important to specify all higher Σ_n according to

$$\Sigma_n(s=0) = 0 \quad \text{for } n \geq 1. \quad (3.12)$$

With Δ_0 and Σ_0 given Δ_1 can be determined algebraically,

$$\Delta_1 = \frac{1}{2} \left(\frac{\bar{\zeta}_0 \sin(\bar{\zeta}_0 s)}{i_0 + \cos(\varphi/2) \cos(\bar{\zeta}_0 s)} \sin(\varphi/2) \right). \quad (3.13)$$

This expression automatically satisfies the initial condition

$$\Delta_1(0) = 0 \quad (3.14)$$

required for the validity of the perturbation expansion. For Σ_1 one obtains the inhomogeneous linear differential equation

$$\dot{\Sigma}_1 + \Sigma_1 \cos \Sigma_0 \cos(\varphi/2) - \Delta_1 \sin \Sigma_0 \sin(\varphi/2) = 0, \quad (3.15)$$

admitting the solution

$$\Sigma_1 = \frac{\tan^2(\varphi/2)}{2(i_0 + \cos(\varphi/2) \cos \bar{\zeta}_0 s)} \left(i_0 \cos(\varphi/2) (1 - \cos \bar{\zeta}_0 s) + \bar{\zeta}_0^2 \ln \frac{i_0 + \cos(\varphi/2) \cos \bar{\zeta}_0 s}{i_0 + \cos(\varphi/2)} \right) \quad (3.16)$$

where we already exploited the initial condition, Eq. 3.12. From Eqs. 3.6, 3.9, 3.13, and 3.16 one derives the normalized voltages

$$v_{1/2} = \frac{\bar{\zeta}_0^2}{i_0 + \cos(\varphi/2) \cos \bar{\zeta}_0 s} + l \frac{\bar{\zeta}_0 \sin(\varphi/2)}{2(i_0 + \cos(\varphi/2) \cos \bar{\zeta}_0 s)^2} \times \quad (3.17)$$

$$\left[\sin(\varphi/2) \sin \bar{\zeta}_0 s \left(i_0 + \cos(\varphi/2) + \frac{\bar{\zeta}_0^2}{\cos(\varphi/2)} \ln \frac{i_0 + \cos(\varphi/2) \cos \bar{\zeta}_0 s}{i_0 + \cos(\varphi/2)} \right) \mp \bar{\zeta}_0 \left(\cos(\varphi/2) + i_0 \cos \bar{\zeta}_0 s \right) \right].$$

In this way we derived an analytic expression for the voltage on junction 1 and 2 resp., valid to first order w.r.t. l . It has to be compared with the solution (2.11) for weakly coupled elements. Both have in common, that there always exists a solution showing phase-locking

for all values of the external field. However, contrary to the case of weak coupling, where the phase shift scales approximately with external flux, we will shortly see that it is negligibly small for all values of the external field, except for $\varphi \approx \pi$. On the other hand, the frequency, being flux-independent for weakly coupled elements, becomes flux-dependent according to Eqs. 3.17,10, detuning the cell this way.

So far, we could not derive an equation of motion (a kind of reduced equation) for the phase shift of strongly coupled elements directly from the basic equations as it is possible for weakly coupled elements. Therefore we must adopt an appropriate alternative definition of phase difference. We define phase shift as the difference of the mean value crossings of the lowest harmonics of v_1 and v_2 according to (3.17).

To proceed, we must evaluate the lowest Fourier coefficients of Eqs. 3.17,

$$v_{1/2} = \frac{\alpha}{2} + a_{1/2} \cos \bar{\zeta}_0 s + b_{1/2} \sin \bar{\zeta}_0 s. \quad (3.18)$$

After some calculation including a Taylor expansion of the logarithm one obtains

$$\alpha = 2\bar{\zeta}_0, \quad (3.19)$$

$$a_{1/2} = \frac{\bar{\zeta}_0}{i_0 + \bar{\zeta}_0} (-2 \cos(\varphi/2) \mp l \bar{\zeta}_0 \sin(\varphi/2)), \quad (3.20)$$

$$b_{1/2} = b = l \frac{\sin^2(\varphi/2) \cos(\varphi/2)}{(i_0 + \bar{\zeta}_0)} \left(1 + \frac{\cos(\varphi/2)}{i_0} + \frac{\bar{\zeta}_0^3}{4i_0^2(i_0 + \bar{\zeta}_0)} \right). \quad (3.21)$$

Note that the Fourier coefficient b being proportional to l is small compared to $a_{1/2}$; the coefficient $a_{1/2}$ itself is dominated by its first term, except for $\varphi = \pi$. Thus, with the possible exception of the vicinity of this value, both voltages are in phase independent of the external flux.

Adopting the definition given before, one can derive a formula for the phase shift δ as a function of the Fourier coefficients,

$$\delta = \arccos \left(\frac{a_1 a_2 + b^2}{\sqrt{b^2(a_1^2 + a_2^2 + b^2) + a_1^2 a_2^2}} \right), \quad (0 \leq \varphi \leq \pi). \quad (3.22)$$

Deriving this formula, no assumption has been made about the structure or order of magnitude of the Fourier coefficients. Extension to $\pi < \varphi \leq 2\pi$ needs a more subtle investigation of the solution itself to get the correct branch of the arccos; in this case one obtains

$$\delta = \text{sgn}(\varphi - \pi) \left[\pi - \arccos \left(\frac{a_1 a_2 + b^2}{\sqrt{b^2(a_1^2 + a_2^2 + b^2) + a_1^2 a_2^2}} \right) \right] + \pi, \quad (3.23)$$

$(0 \leq \varphi \leq 2\pi).$

Fig. 3 shows the phase shift between v_1 and v_2 as a function of external flux φ .

Our analytical approach was accompanied by numerical investigations exploiting the Personal Superconducting Circuit ANalyzer program PSCAN^{32,33} (Fig. 4). Comparison of Figs. 3 and 4 shows that even for $l = 1$ where the analytical approximation is not longer valid results are quite similar to those of the numerical simulation. Both figures show that already in this case the behavior is qualitatively different from that of weakly coupled elements. Thus, in the intermediate regime $l \approx 1$ the strong coupling scheme provides a better approximation to the actual behavior of the SQUID cell than the weak coupling results do.

There are two limiting cases of special interest. For vanishing external flux the elements behave in the same way as one junction; the phase shift between voltages vanishes and the elements oscillate with voltages

$$v_1 = v_2 = \frac{\zeta_0^2}{i_0 + \cos \zeta_0 s}. \quad (3.24)$$

This behavior is plausible, because in this case there is no current flowing through the shunt and both elements act essentially as one element. For $\varphi = \pi$ one obtains

$$v_1 = i_0 - \frac{l i_0}{2} \sin i_0 s + \frac{l}{4} \sin 2i_0 s, \quad (3.25)$$

$$v_2 = i_0 + \frac{l i_0}{2} \sin i_0 s + \frac{l}{4} \sin 2i_0 s. \quad (3.26)$$

This clearly indicates that the phase difference δ between the voltages according to our definition is equal to π . Within the narrow transition region between the regimes $\delta \approx 0$ and $\delta \approx \pi$ oscillations become highly non-harmonic (cf. the voltages in Figs. 5a and 5b). This is caused by higher harmonics becoming dominant in comparison to the lowest harmonic with frequency $\bar{\zeta}_0$. In this case the definition of phase difference based on the lowest harmonic of the Fourier expansion (3.18) as well in the analytical calculation as in the numerical

procedure becomes less reliable. The jump observed in the numerical curve (Fig. 4) may be assigned to this fact.

To derive a more simple rule of thumb Eq. 3.22 can be rewritten as

$$\delta(\varphi) = \arctan(a_2/b) - \arctan(a_1/b), \quad 0 \leq \varphi < \pi. \quad (3.27)$$

with $a_{1/2}$ and b according to (3.20,3.21). We consider this formula for very small, but finite l . In this case, the second arctan approaches the value $-\pi/2$. The first one changes its sign at the flux φ^* ,

$$\cos(\varphi^*/2) - \frac{l}{2}\zeta_0 \sin(\varphi^*/2) = 0. \quad (3.28)$$

Exploiting this formula while neglecting higher orders in l , one obtains

$$\varphi^* \approx \pi - i_0 l. \quad (3.29)$$

This provides a simple approximation for the phase shift of the cells under investigation,

$$\delta \approx \pi \theta(\varphi - \varphi^*) \quad (\varphi \leq \pi). \quad (3.30)$$

Fig. 6 shows that for sufficiently small l the solution is indeed perfectly approximated by a Heaviside step function. This approximation might be useful considering more complicated arrays.

Another quantity of interest is the I - V characteristics of the cells under investigation. From (3.18) one easily obtains

$$\bar{v}_{1/2} = \sqrt{i_0^2 - \cos^2(\varphi/2)}. \quad (3.31)$$

This reproduces a well-known result³: The I - V characteristics of a small-inductance SQUID has a hyperbolic shape, the vertex being dependent on the external flux.

IV. PARAMETER-SPLITTING IN STRONGLY COUPLED CELLS

Real junctions never have identical parameters. The response to parameter differences becomes particularly important in large arrays, where one usually cannot avoid a parameter-

splitting of the order of one p.c., at least. In this section we consider junctions having different critical currents as well as normal resistances,

$$I_{C_1} \neq I_{C_2}, \quad R_{N_1} \neq R_{N_2}, \quad (4.1)$$

with the subsidiary condition

$$I_{C_1} R_{N_1} = I_{C_2} R_{N_2}, \quad (4.2)$$

which is usually realized as a consequence of the technological process with a good accuracy.

Introducing the mean critical current

$$I_C = \frac{1}{2}(I_{C_1} + I_{C_2}) \quad (4.3)$$

and the parameter-splitting

$$\vartheta = \frac{I_{C_2} - I_{C_1}}{I_{C_2} + I_{C_1}}, \quad (4.4)$$

one derives the following RSJ-model equations for the cells shown in Fig. 1:

$$\dot{\phi}_1 + \sin \phi_1 = \frac{i_0}{1 - \vartheta} - \frac{1}{l(1 - \vartheta)}(\phi_1 - \phi_2 + \varphi), \quad (4.5a)$$

$$\dot{\phi}_2 + \sin \phi_2 = \frac{i_0}{1 + \vartheta} + \frac{1}{l(1 + \vartheta)}(\phi_1 - \phi_2 + \varphi). \quad (4.5b)$$

As before, it is advantageous to introduce new variables Δ and Σ according to Eq. 3.1.

Eqs. 3.2a,b are then modified to

$$\dot{\Delta} + \cos \Sigma \sin \Delta = -\frac{\vartheta}{1 - \vartheta^2} i_0 + \frac{1}{l(1 - \vartheta^2)}(\varphi - 2\Delta), \quad (4.6a)$$

$$\dot{\Sigma} + \sin \Sigma \cos \Delta = \frac{1}{1 - \vartheta^2} i_0 - \frac{\vartheta}{l(1 - \vartheta^2)}(\varphi - 2\Delta). \quad (4.6b)$$

Some effects are already qualitatively displayed by this couple of equations. (i) To first order in ϑ there is a correction of the magnetic flux $\sim -i_0 l \vartheta$. (ii) There is a correction of the bias current $\vartheta(\varphi - 2\Delta)/l$ being of first order, too. It includes an additional coupling via Δ . Eqs. (4.6a,b) indicate that for weak coupling ($l \gg 1, \vartheta \ll 1$) the additional magnetic flux dominates, an effect which has already been observed (cf. Eq. 13.30b in³). However,

for strong coupling ($l \ll 1, \vartheta \ll 1$) this term is of second order only. It turns out that the difference $\varphi - 2\Delta$ is of the order of l , so the addition to the bias current is of first order in ϑ and dominates.

First of all, we are interested in the maximum parameter-splitting which is possible without destroying synchronization. For this purpose, the splitting-parameter ϑ should not be considered small from the beginning. As before, we perform a perturbation expansion w.r.t. l according to (3.3a,3.3b). To lowest, i.e. -1^{st} , order we again obtain $\Delta_0 = \varphi/2$. To 0^{th} order, we get the system of equations

$$\dot{\Sigma}_0 + \sin \Sigma_0 \cos(\varphi/2) = \frac{i_0}{1 - \vartheta^2} + \frac{2\vartheta}{1 - \vartheta^2} \Delta_1, \quad (4.7a)$$

$$\cos \Sigma_0 \sin \Delta_0 = -\frac{\vartheta}{1 - \vartheta^2} i_0 - \frac{2}{1 - \vartheta^2} \Delta_1. \quad (4.7b)$$

Again, Σ_0 has to be determined by solving a differential equation, whereas Δ_1 is calculated algebraically. The new feature is an additional coupling between both variables caused by the last term on the r.h.s. of Eq. 4.7a. Combining both equations, one obtains

$$\dot{\Sigma}_0 + \sin \Sigma_0 \cos(\varphi/2) + \vartheta \cos \Sigma_0 \sin(\varphi/2) = \frac{i_0}{1 - \vartheta^2}. \quad (4.8)$$

In comparison to (3.8) this equation shows an additional non-linearity due to the parameter-splitting. Moreover, the current is divided by $(1 - \vartheta^2)$, indicating that a splitting of critical current can lower the current necessary for the onset of oscillations.

Eq. 4.8 can be handled exactly. There are four different types of solutions³⁴. Only one of them shows the continuous transition to the case $\vartheta = 0$ and the corresponding oscillating voltage: It is realized for

$$\frac{i_0^2}{1 - \vartheta^2} > \vartheta^2 \sin^2(\varphi/2) + \cos^2(\varphi/2). \quad (4.9)$$

Further estimation gives the bound for oscillations to occur,

$$i_0^2 > 1 - \vartheta^2. \quad (4.10)$$

For $\vartheta = 0$ this reproduces a well-known fact. In addition, it proves the conjecture above that growing parameter-splitting leads to an effective lowering of the critical current.

With this condition fulfilled we could evaluate Σ_0 and from (4.7b) Δ_1 . However, although Σ_1 has to be determined from a first-order linear differential equation, the resulting integrals are rather intricate. Thus, we performed a perturbative treatment of the system (4.6a,b) not only w.r.t. l , but w.r.t. ϑ , too. This is more delicate, of course, because there are two parameters involved. To discuss the l - and ϑ -dependence independently, it's not wise to specify the ratio l/ϑ from the beginning. We only suppose $l \ll 1$ and $\vartheta \ll 1$, leaving the ratio ϑ/l unspecified. To first order, we write down the expansion

$$\Delta = \Delta_0 + l\Delta_{10} + \vartheta\Delta_{01}, \quad (4.11a)$$

$$\Sigma = \Sigma_0 + l\Sigma_{10} + \vartheta\Sigma_{01}. \quad (4.11b)$$

Inserting into (4.6a,b) and comparing equal orders $l^m\vartheta^n$, one obtains the set of equations necessary to evaluate the Δ 's and Σ 's. For $\Delta_0, \Sigma_0, \Delta_{10}$, and Σ_{10} one obtains similar equations as before. Furthermore, one observes $\Delta_{01} = 0$; thus, no additional phase shift is caused by the parameter-splitting. For Σ_{01} one obtains an equation similar in structure to that for Σ_{10} (cf. Eq. 3.15),

$$\dot{\Sigma}_{01} + \Sigma_{01} \cos \Sigma_0 \cos(\varphi/2) + \cos \Sigma_0 \sin(\varphi/2) = 0. \quad (4.12)$$

It admits the solution

$$\Sigma_{01} = \frac{1 - \cos \bar{\zeta}_0 s}{i_0 + \cos(\varphi/2) \cos \bar{\zeta}_0 s} \sin(\varphi/2). \quad (4.13)$$

Thus, weak parameter-splitting leads to an additional in-phase contribution

$$\vartheta(i_0 + \cos(\varphi/2)) \sin \bar{\zeta}_0 s \frac{\bar{\zeta}_0 s \sin(\varphi/2)}{(i_0 - \cos(\varphi/2) \cos \bar{\zeta}_0 s)^2} \quad (4.14)$$

to be added to the voltages (3.17). The Fourier coefficients $a_{1/2}$ are unaffected by this, whereas there is an additional contribution to $b_{1/2}$,

$$b_{1/2}^\vartheta = 2\vartheta(i_0 + \cos(\varphi/2)) \frac{\sin(\varphi/2)}{i_0 + \bar{\zeta}_0}. \quad (4.15)$$

The solution obtained this way proves our earlier conjecture on the dominant contribution in the strong-coupling case (Fig. 7a). One observes that the phase shift, being slightly raised

generally is considerably lowered for $\varphi = \pi$. To lowest order of our analytic approximation (valid for strong coupling and weak parameter splitting) there is no indication of a shift of the peak caused by the parameter splitting. This is confirmed by comparison with numerical simulation, as long as parameter splitting is sufficiently small ($\vartheta \lesssim 0.2$). For larger ϑ the numerical result (Fig. 7b) gives a first hint to the peak shift.

V. CAPACITIVELY SHUNTED JUNCTIONS

The influence of the displacement current flowing through the junctions was neglected up to now. This is justified, as long as the McCumber parameter^{35,36}

$$\beta = \frac{2e}{\hbar} I_C R_N^2 C \quad (5.1)$$

is negligible.

In this section, we will investigate the influence of $\beta \neq 0$. The displacement current adds a second-derivative term to the RSJ model equations (sometimes called RCSJ model equations then),

$$\beta \ddot{\phi}_1 + \dot{\phi}_1 + \sin \phi_1 = i_0 - l^{-1}(\phi_1 - \phi_2 + \varphi), \quad (5.2a)$$

$$\beta \ddot{\phi}_2 + \dot{\phi}_2 + \sin \phi_2 = i_0 + l^{-1}(\phi_1 - \phi_2 + \varphi). \quad (5.2b)$$

In general, the second derivative may change the character of the differential equations completely; for instance, it is well-known that there appear new types of solutions showing chaotic behavior^{37,38}. Here, we will restrict our treatment to small β ($\beta \ll 1$) guaranteeing a continuous transition to the former solution for $\beta = 0$.

Again, it is recommended to combine Eqs. 5.2a,b obtaining

$$\beta \ddot{\Delta} + \dot{\Delta} + \cos \Sigma \sin \Delta = \frac{1}{l}(\varphi - 2\Delta), \quad (5.3a)$$

$$\beta \ddot{\Sigma} + \dot{\Sigma} + \sin \Sigma \cos \Delta = i_0. \quad (5.3b)$$

One clearly sees, that both equations are affected by the additional β -terms. Again, both l and β are supposed to be small parameters justifying the expansion

$$\Delta = \Delta_0 + l\Delta_{10} + \beta\Delta_{01}, \quad (5.4a)$$

$$\Sigma = \Sigma_0 + l\Sigma_{10} + \beta\Sigma_{01}. \quad (5.4b)$$

The resulting equations for $\Delta_0, \Sigma_0, \Delta_{10}$, and Σ_{10} , resp., are essentially the same as before.

For Δ_{01} one readily recovers

$$\Delta_{01} = 0. \quad (5.5)$$

The only new equation concerns Σ_{01} ,

$$\dot{\Sigma}_{01} + \Sigma_{01} \cos \Sigma_0 \cos(\varphi/2) = -\ddot{\Sigma}_0, \quad (5.6a)$$

where we have already exploited some of the previous results. Again, this is an inhomogeneous linear differential equation, with the inhomogeneity being determined by the already well-known Σ_0 . The solution, obeying the correct boundary condition ($\Sigma_{01}(s=0) = 0$), is

$$\Sigma_{01} = \frac{\bar{\zeta}_0^2}{i_0 - \cos(\varphi/2) \cos \bar{\zeta}_0 s} \ln \frac{i_0 + \cos(\varphi/2) \cos \bar{\zeta}_0 s}{i_0 + \cos(\varphi/2)}. \quad (5.7)$$

One obtains a logarithmic structure similar to that observed earlier in formula (3.16). The term (5.7) provides to both voltages a contribution

$$\dot{\Sigma}_{01} = \frac{\bar{\zeta}_0^3 \cos(\varphi/2) \sin \bar{\zeta}_0 s}{(i_0 + \cos(\varphi/2) \cos \bar{\zeta}_0 s)^2} \left(\ln \frac{i_0 + \cos(\varphi/2) \cos \bar{\zeta}_0 s}{i_0 + \cos(\varphi/2)} - 1 \right). \quad (5.8)$$

Because the logarithmic structure is already present in (3.17), it is not hard to evaluate the corresponding capacitive contribution to be added to the Fourier coefficients $b_{1/2}$ according to (3.21),

$$b_{1/2}^\beta = b^\beta = -2\beta\bar{\zeta}_0^2 \frac{\cos(\varphi/2)}{(i_0 + \bar{\zeta}_0)} \left(1 + \frac{\cos(\varphi/2)}{i_0} - \frac{\bar{\zeta}_0 \cos^2(\varphi/2)}{4i_0^2(i_0 + \bar{\zeta}_0)} \right). \quad (5.9)$$

The phase difference obtained by inserting (3.21) and (5.9) together with the unchanged coefficients (3.20) into (3.23) is shown in Fig. 8a. Results of a numerical calculation performed in parallel are given in Fig. 8b. The general tendency is that a non-vanishing capacitance ($\beta \lesssim 1$) slightly enhances the phase shift without qualitatively changing the general behavior. For $\beta > 0.5$ the agreement between analytical approximation and numerical simulation becomes worse, but the same general tendency is still preserved. This is, of course, simply a result of the fact that higher orders in β are no longer negligible.

VI. STRONGLY COUPLED SQUID CELLS UNDER MICROWAVE RADIATION

There is some interest in the behavior of the SQUID cells under microwave radiation from at least two points of view. First of all, the topic is interesting for the construction of sensitive microwave detectors. Secondly, knowledge of the behavior under microwave radiation is necessary for the study of synchronization in larger arrays, where the long-range interaction via external shunts acts similar to an external microwave signal.

The external microwave signal can be described by an additional ac current, leading to the system of equations

$$\dot{\phi}_1 + \sin \phi_1 = i_0 - l^{-1}(\phi_1 - \phi_2 + \varphi) + i_\omega \sin \omega s, \quad (6.1a)$$

$$\dot{\phi}_2 + \sin \phi_2 = i_0 + l^{-1}(\phi_1 - \phi_2 + \varphi) + i_\omega \sin \omega s. \quad (6.1b)$$

As a result, only the equation for the sum variable Σ is affected and becomes

$$\dot{\Sigma} + \sin \Sigma \cos \Delta = i_0 + i_\omega \sin \omega s, \quad (6.2)$$

whereas Eq. 3.2a for the difference variable Δ remains unchanged. We apply a perturbation scheme similar to that used before. From the beginning we will assume $l \ll 1$, as before, justifying the expansion (3.3a,b). Solving for Σ_0 and Σ_1 , resp., we must take i_ω to be small in some intermediate steps, too.

The first result is

$$\Delta_0 = \varphi/2, \quad (6.3)$$

as usual. The corresponding equation for Σ_0 ,

$$\dot{\Sigma}_0 + \sin \Sigma_0 \cos(\varphi/2) = i_0 + i_\omega \sin \omega s, \quad (6.4)$$

is decisive for the behavior of the solution. Introducing the scaled time \tilde{s} according to (3.7), we obtain

$$\Sigma'_0 + \sin \Sigma_0 = \tilde{i}_0 + \tilde{i}_\omega \sin \tilde{\omega} \tilde{s}, \quad \tilde{i}_\omega = \frac{i_\omega}{\cos(\varphi/2)}, \quad \tilde{\omega} = \frac{\omega}{\cos(\varphi/2)}, \quad (6.5)$$

which formally has the same structure as the equation describing an autonomous Josephson junction under external irradiation^{26,31,39}.

It is well-known that phase-locking of an autonomous junction takes place only if the frequency of the external microwave does not deviate too far from the inherent Josephson frequency $\zeta_0 = \sqrt{i_0^2 - 1}$,

$$\left| \frac{2\zeta_0}{i_\omega}(\omega - \zeta_0) \right| < 1 \quad (\text{autonomous contact}). \quad (6.6)$$

The main new feature in our case is, that the corresponding quantities substituted for i_0, i_ω , and ω resp. according to

$$i_0 \rightarrow \tilde{i}_0, \quad (6.7)$$

$$i_\omega \rightarrow \tilde{i}_\omega, \quad (6.8)$$

$$\omega \rightarrow \tilde{\omega} \quad (6.9)$$

are dependent on the external magnetic flux. Exploiting the corresponding equation

$$\left| \frac{2\tilde{\zeta}_0}{\tilde{i}_\omega}(\tilde{\omega} - \tilde{\zeta}_0) \right| < 1, \quad (6.10)$$

one obtains the phase-locking condition

$$\bar{\zeta}_0 - \frac{i_\omega \cos(\varphi/2)}{2\bar{\zeta}_0} \leq \omega \leq \bar{\zeta}_0 + \frac{i_\omega \cos(\varphi/2)}{2\bar{\zeta}_0}. \quad (6.11)$$

An interesting conclusion from Eq. 6.11 is that for external flux $\varphi = \pi$ the range of phase-locking shrinks to a single point, $\omega = \bar{\zeta}_0 = i_0$. In this case, for all practical purposes phase-locking disappears at all. This is confirmed by Fig. 9, showing the range of phase-locking against external flux φ . The reason for this behavior is obvious from examining (6.4): For $\varphi = \pi$ the non-linear term vanishes thus removing the non-linearity of the equation at all. One more observation is that the center of the locking-range determined by $\bar{\zeta}_0$ becomes flux-dependent, too.

In case of phase-locking, phase shift between the external microwave and the circuit (the last being characterized by the sum variable Σ) can be deduced from comparison with the autonomous contact yielding

$$\delta_0 = \arcsin \frac{2\bar{\zeta}_0(\omega - \bar{\zeta}_0)}{i_\omega \cos(\varphi/2)}. \quad (6.12)$$

To verify our result in an independent way, we performed a numerical operation range analysis automatically integrating the corresponding differential equations and checking, whether the results lie within a certain bound. The output of this analysis indicated by diamonds in Fig. 9 is in excellent agreement with the analytical results. In view of the experimental setup the figure should be interpreted as follows: For a fixed bias current and frequency of the external microwave radiation there is a limited range of flux indicated in Fig. 9, within which synchronization occurs. Within this range the whole cell oscillates with the microwave frequency, ω . For small microwave intensities this puts rather severe conditions on the external flux, as is observed by comparing Figs. 9a, b and c.

In case of phase-locking, we obtain to 0^{th} order of perturbation theory

$$\Sigma_0 = 2 \arctan \left(\frac{\bar{\zeta}_0}{i_0 + \cos(\varphi/2)} \tan \left(\frac{\omega s}{2} - \frac{\delta_0}{2} \right) \right) + \frac{\pi}{2} \quad (6.13)$$

with the lowest-order phase shift δ_0 according to (6.12).

Within the next perturbative order, Δ_1 is determined algebraically as before. The solution is identical to Eq. 3.13, the only difference being, that within the time-dependent arguments one has to substitute

$$\bar{\zeta}_0 s \rightarrow \omega s - \delta_0. \quad (6.14)$$

For Σ_1 we obtain the equation

$$\dot{\Sigma}_1 + \Sigma_1 \cos \Sigma_0 \cos(\varphi/2) - \Delta_1 \sin \Sigma_0 \sin(\varphi/2) = 0. \quad (6.15)$$

Substituting Σ_0 we exploit (6.4) neglecting the external current, bearing in mind that i_ω is small and Σ_1 is already of first order. Within this approximation, the solution has the same general structure as (3.16), where we again have to substitute (6.14). As a result, in addition to the flux-dependent phase shift between the SQUID circuit voltage oscillations and the external microwave signal we obtain the same (mostly negligible) phase splitting between the junction voltages than without radiation.

To summarize, solution (3.17) is reproduced with the only substitution (6.14). This has several consequences: (i) The frequency of the oscillations is determined by the microwave frequency only and turns out to be independent of external flux within the locking-range. (ii) If external flux is present in addition to the microwave radiation, this flux will limit the range of phase-locking in general and destroy synchronization at all in case of $\varphi = \pi$. (iii) The relative phase of both junctions is not influenced by the external radiation up to first order in perturbation theory w.r.t. l . (iv) There is an additional shift of both phases relative to the external radiation according to Eq. 6.12, which is controlled by external flux as well.

VII. SUMMARY

We investigated the synchronization behavior of three similar 2-junction SQUID cells with strong inductive coupling. For this purpose we developed a perturbation scheme appropriate for small but non-vanishing inductances. The perturbation ansatz itself is in a certain sense similar to the "slowly-varying amplitude method" developed several years ago. However, application to strong coupling completely changes the character of the expansion. Generally, the procedure is more involved than in the case of weak coupling. Therefore we were not able to derive an explicit equation of motion for the phase difference between voltages. In view of this fact, we determined voltage phase shift from the lowest Fourier coefficients of the voltages.

For identical junctions without capacitive shunting we find that for every value of the external flux a phase-locking between oscillating voltages takes place like in weakly coupled elements. However, contrary to the case of weak coupling, the phase shift is negligibly small for almost all values of external flux, with the exception of the vicinity of $\varphi = \pi$. On the other hand, the frequency, being flux-independent for weakly coupled elements, becomes strongly flux-dependent in strongly coupled elements and, consequently, the corresponding I - V characteristics too. The results obtained are compared with numerical calculations. Generally, a good agreement is observed. Especially it is found, that the strong-coupling

approach provides a good approximation not only for very small inductances l , but is better suited to describe the intermediate range $l \approx 1$ than the ordinary weak-coupling approach.

If both junctions are not identical the influence of parameter splitting is found to be qualitatively different for weak and for strong coupling. For weak coupling, parameter splitting mainly leads to an additional contribution to the external flux; as a result, the whole phase-flux-dependence is shifted by some value. In case of strong coupling, this effect can be neglected and the leading contribution is a correction of the bias current. This correction acts in favor of synchronization and lowers the phase shift present in a small range around $\varphi = \pi$.

In case of identical junctions having a small, but non-vanishing capacitance the main result is a slight enhancement of the phase shift, although the qualitative picture is not changed, at least if $\beta < 1$. For $\beta > 0.5$ the agreement of analytical results and numerical simulation becomes less convincing, obviously showing the limitations of applicability of the analytical perturbative method. We should mention that in the case $\beta \neq 0$ as well as for parameter splitting two independent expansion parameters must be considered small.

Finally, we investigated the behavior of the cells under external microwave radiation. In this case, we observed a limited locking range similar to that of an autonomous Josephson junction under external radiation. However, for a strongly coupled cell the synchronization range is flux-dependent and shrinks to zero for $\varphi = \pi$. In addition, the width of the synchronization range depends on the amplitude of the external radiation.

Contrary to our results for a freely oscillating cell, external radiation synchronizes the cell in such a way that the oscillation frequency becomes flux-independent within the flux-dependent locking range. However, within the synchronization range, an additional phase shift between external radiation and internal oscillations takes place as well as a shift of the whole synchronization range.

From our study one can draw the general conclusion, that two strongly inductive coupled junctions behave like a free junction if no flux is present within the cell. External flux tends to shift the phases between the voltage oscillations of the two junctions, but for most

practical applications this splitting is negligibly small. More serious is the fact that already in a cell of identical junctions the oscillation frequency itself becomes field-dependent. This detuning of the cell has several consequences for the construction of larger arrays. First of all, external fluxes must be shielded, preferably by an external superconducting ground plane. Secondly, additional fluxes are produced by the array itself, which might seriously disturb the synchronization⁴⁰.

A possible way to circumvent this problem and to obtain phase-locking could be to include an external long-range interaction via an additional shunt. The methods developed in Sec. VI could be helpful in such an investigation. For instance, according to our observations, an external shunt with sufficiently strong coupling-strength to make the synchronization frequency flux-independent may play a crucial role for obtaining phase-locking in large two-dimensional arrays.

ACKNOWLEDGMENTS

This work was supported by a project of the BMBW under contract # 13N6132 and by DFG under contract # KR1172/4-1. The authors would like to express their thanks to BMBW, DFG and DAAD for financial support. In addition, the authors would like to thank A. Nowack for a critical reading of the manuscript.

FIGURES

FIG. 1. Three SQUID Cells which can be described with the strong coupling method described in this paper.

FIG. 2. Mean voltage phase shift δ against normalized external flux φ from analytical approximation for weak inductive coupling ($i_0 = 1.5$).

FIG. 3. Phase shift δ against normalized external flux φ for strong inductive coupling $l = 0.1$ and medium inductive coupling $l = 1.0$ obtained from analytical approximation (3.23) ($i_0 = 1.5$).

FIG. 4. Like Fig. 3, results obtained from numerical simulation. (A tiny shunt capacitance $\beta = 0.01$ has to be added here.)

FIG. 5. Time-dependence of the voltage for two different values of the external flux, a) $\varphi = \pi/2$ b) $\varphi = \pi$, Parameters: $i_0 = 1.5$, $l = 0.1$.

FIG. 6. Phase shift δ against normalized external flux φ for extremely strong coupling ($0.001 \leq l \leq 0.1$), obtained from analytical approximation (3.23) ($i_0 = 1.5$).

FIG. 7. The influence of parameter splitting on the phase shift δ against normalized external flux φ for strong coupling obtained from a) analytical approximation (3.23), b) numerical simulation ($i_0 = 1.5$, $l = 0.1$, $2 \leq \varphi \leq 4$).

FIG. 8. The influence of a non-vanishing capacitive shunt of the Josephson junctions on the phase difference for $i_0 = 1.5$, $l = 0.1$, $\beta = 0.2, 0.5, 1.0$. a) analytical approximation, b) numerical simulation ($i_0 = 1.5$, $l = 0.1$, $2 \leq \varphi \leq 4$).

FIG. 9. Synchronization range for a strongly coupled SQUID cell under external microwave radiation with frequency ω for a) $i_\omega = 0.1$, b) $i_\omega = 0.2$, c) $i_\omega = 0.4$ (bias current $i_0 = 1.5$). The diamonds indicate results from numerical operation range analysis.

REFERENCES

- ¹ A. K. Jain, K. K. Likharev, J. E. Lukens, and J. E. Sauvageau, *Phys. Rep.* **109**, 310 (1984).
- ² J. B. Hansen and P. E. Lindelof, *Rev. Mod. Phys.* **56**, 431 (1984).
- ³ K. K. Likharev, *Dynamics of Josephson junctions and circuits* (Gordon and Breach, Philadelphia, 1991).
- ⁴ S. P. Benz and C. J. Burroughs, *Supercond. Sci. Technol.* **4**, 561 (1991).
- ⁵ S. P. Benz and C. J. Burroughs, *Appl. Phys. Lett.* **58**, 2162 (1991).
- ⁶ P. E. Lindelof and J. B. Hansen, *Rev. Mod. Phys.* **56**, 431 (1984).
- ⁷ J. E. Lukens, A. K. Jain, and K.-L. Wan, in *Proceedings of the NATO Advanced Study Institute on Superconducting Electronics*, edited by M. Nisenoff and H. Weinstock (Springer, Heidelberg, 1989), pp. 235–258.
- ⁸ J. E. Lukens, in *Superconducting Devices*, edited by S. T. Ruggiero and D. A. Rudman (Academic Press, New York, 1990), pp. 135–167.
- ⁹ J. Konopka, in *Weak Superconductivity*, edited by S. Benacka, P. Seidel, and V. Strbik (Institute of Electrical Engineering, Slovak Academy of Sciences, Bratislava, 1994), pp. 221–232.
- ¹⁰ W. Krech, *Ann. Phys. (Leipzig)* **39**, 117 (1982).
- ¹¹ W. Krech, *Ann. Phys. (Leipzig)* **39**, 349 (1982).
- ¹² P. Hadley, M. R. Beasley, and K. Wiesenfeld, *Appl. Phys. Lett.* **52**, 1619 (1988).
- ¹³ K. Wan, A. K. Jain, and J. E. Lukens, *Appl. Phys. Lett.* **54**, 1805 (1989).
- ¹⁴ S. Han, B. Bi, W. Zhang, and J. E. Lukens, in *Proceedings of the Fourth International Superconductive Electronics Conference (ISEC '93)*, (Boulder, 1993), pp. 335–336.

- ¹⁵ S. Han, B. Bi, W. Zhang, and J. E. Lukens, *Appl. Phys. Lett.* **64**, 11 (1994).
- ¹⁶ P. A. A. Booij *et al.*, *IEEE Trans. Appl. Supercond.* **3**, 2493 (1993).
- ¹⁷ J. S. Martens *et al.*, in *Proceedings of the Fourth International Superconductive Electronics Conference (ISEC '93)*, (Boulder, 1993), pp. 361–362.
- ¹⁸ J. A. Stern, H. G. LeDuc, and J. Zmudzinis, *Trans. Appl. Supercond.* **3**, 2485 (1993).
- ¹⁹ B. Liu, and J. Wengler, in *Proceedings of the Fourth International Superconductive Electronics Conference (ISEC '93)*, (Boulder, 1993), pp. 357–358.
- ²⁰ T. Doderer *et al.*, in *Applied Superconductivity Conference 1994, to App. In Proceedings* (Boston, 1994).
- ²¹ R. L. Kautz, in *Applied Superconductivity Conference 1994, to App. In Proceedings* (Boston, 1994).
- ²² K. K. Likharev, L. S. Kuzmin, and G. A. Ovsyannikov, *IEEE Trans. Magn.* **17**, 111 (1981).
- ²³ L. S. Kuzmin, K. K. Likharev, and G. A. Ovsyannikov, *Radio Eng. and Electr.* **26**, 102 (1981).
- ²⁴ W. Krech and H.-H. Große, *Ann. Phys. (Leipzig)* **35**, 207 (1978).
- ²⁵ W. Krech, *Ann. Phys (Leipzig)* **39**, 50 (1982).
- ²⁶ W. Krech, *Wiss. Z. FSU Jena, Math.-Nat. R.* **32**, 19 (1983).
- ²⁷ A. F. Volkov and F. V. Nad', *JETP Lett.* **11**, 56 (1970).
- ²⁸ M. J. Stephen, *Phys. Rev.* **186**, 393 (1970).
- ²⁹ L. L. Sohn *et al.*, *Phys. Rev. B* **47**, 975 (1993).
- ³⁰ M. Basler, W. Krech, and K. Y. Platov, *Phys. Lett. A* **190**, 489 (1994).
- ³¹ E. D. Thompson, *J. Appl. Phys* **44**, 5587 (1973).

- ³² A. A. Odintsov, V. K. Semenov, and A. B. Zorin, *IEEE Trans. Magn.* **23**, 763 (1987).
- ³³ S. V. Polonsky, V. K. Semenov, and P. N. Shevchenko, in *Proc. ISEC'91* (Scotland, 1991).
- ³⁴ I. S. Gradshteyn and I. M. Ryzhik, *Tables of Series, Products and Integrals* (Verlag Harri Deutsch, Thun, Frankfurt/M, 1981).
- ³⁵ D. E. McCumber, *J. Appl. Phys.* **39**, 3113 (1968).
- ³⁶ W. C. Steward, *Appl. Phys. Lett.* **12**, 277 (1968).
- ³⁷ P. M. Marcus, Y. Imry, and E. Ben-Jacob, *Solid State Commun.* **41**, 161 (1982).
- ³⁸ R. F. Miracky, J. Clarke, and R. H. Koch, *Phys. Rev. Lett.* **50**, 856 (1983).
- ³⁹ K. K. Likharev and L. S. Kuzmin, *Radiotekhnika i elektronika* **22**, 1689 (1977).
- ⁴⁰ J. Phillips, H. V. der Zant, J. White, and T. Orlando, *Phys. Rev. B* **47**, 5219 (1993).

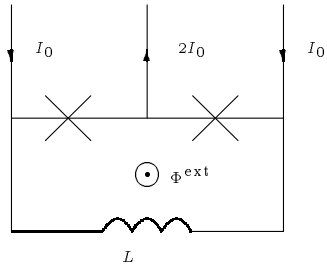


Fig. 1a

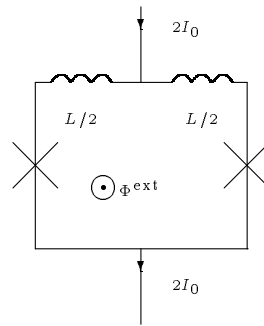


Fig. 1b

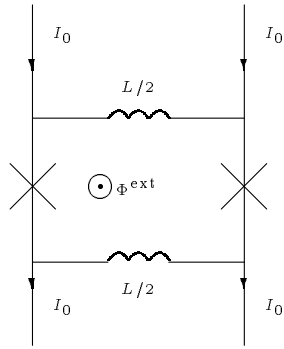


Fig. 1c

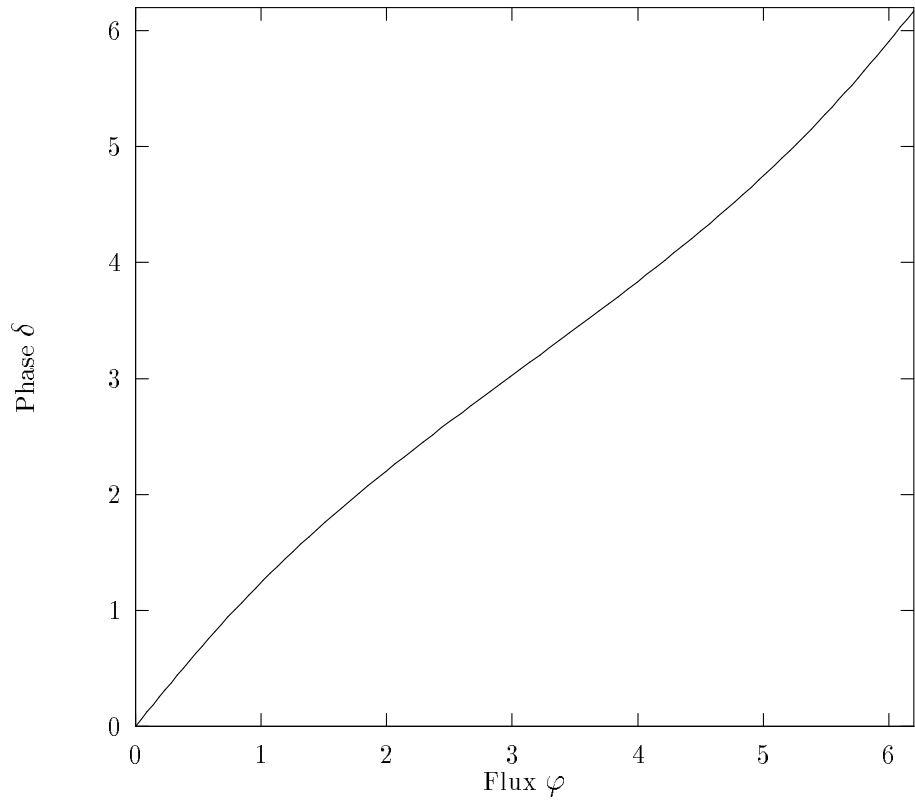


Fig. 2

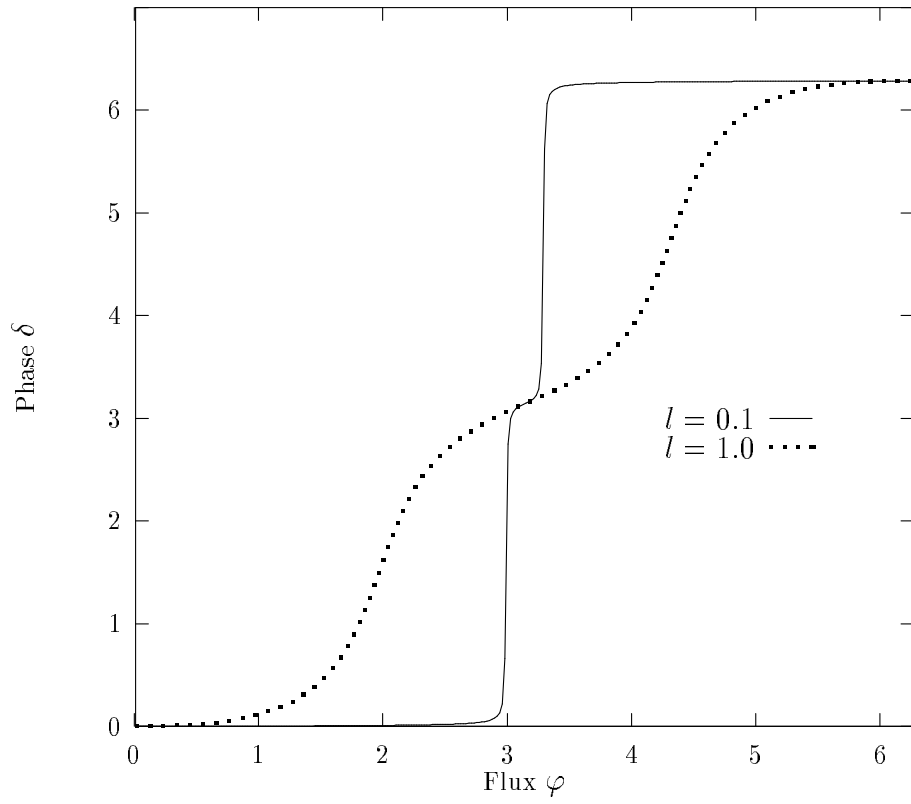


Fig. 3

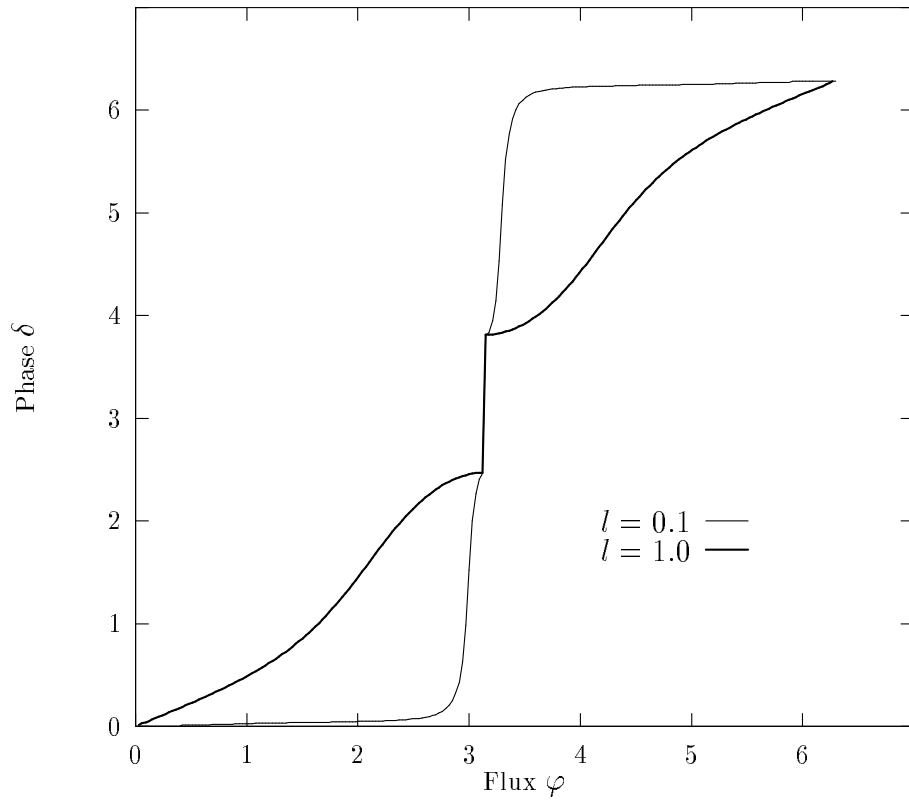


Fig. 4

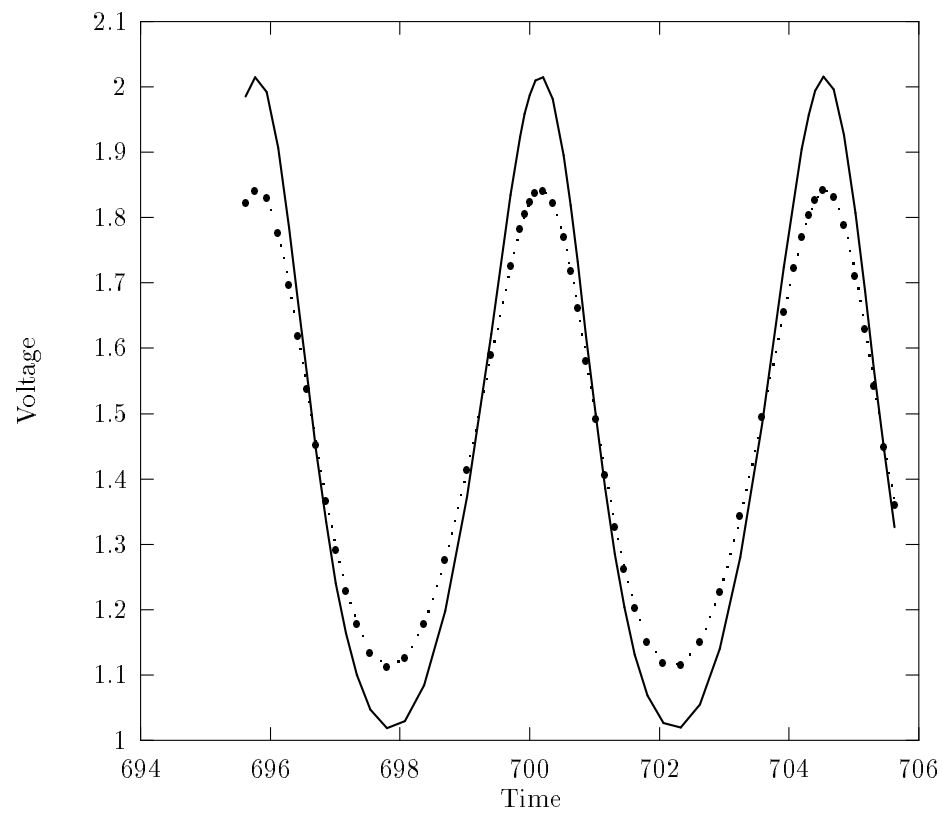


Fig. 5a

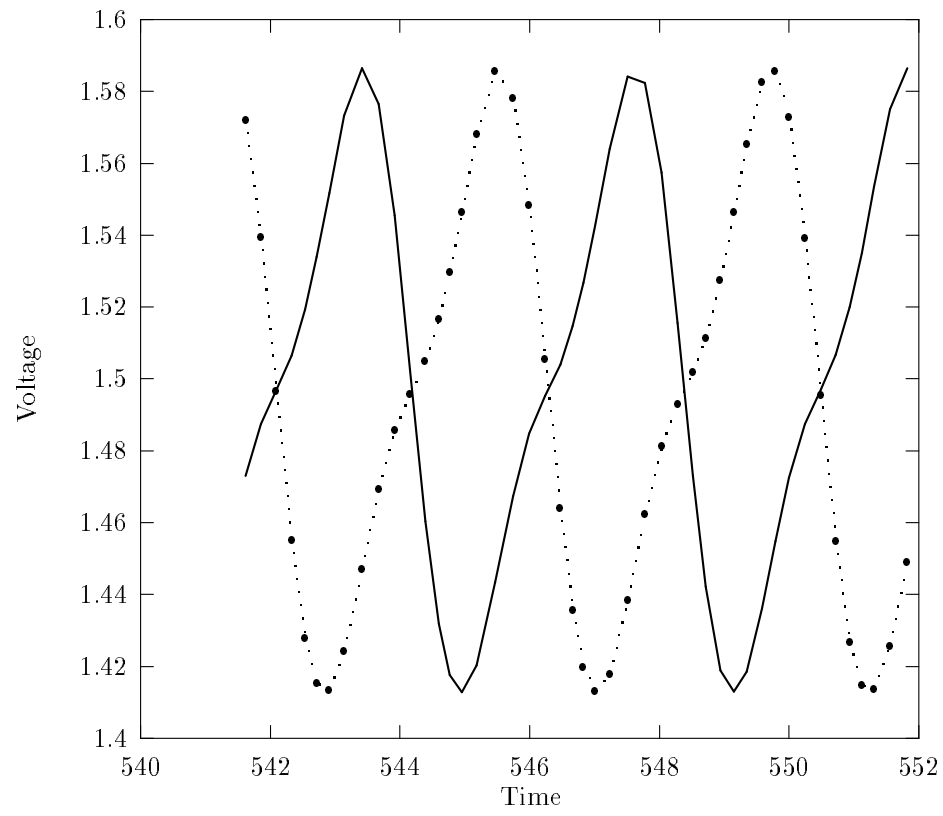


Fig. 5b

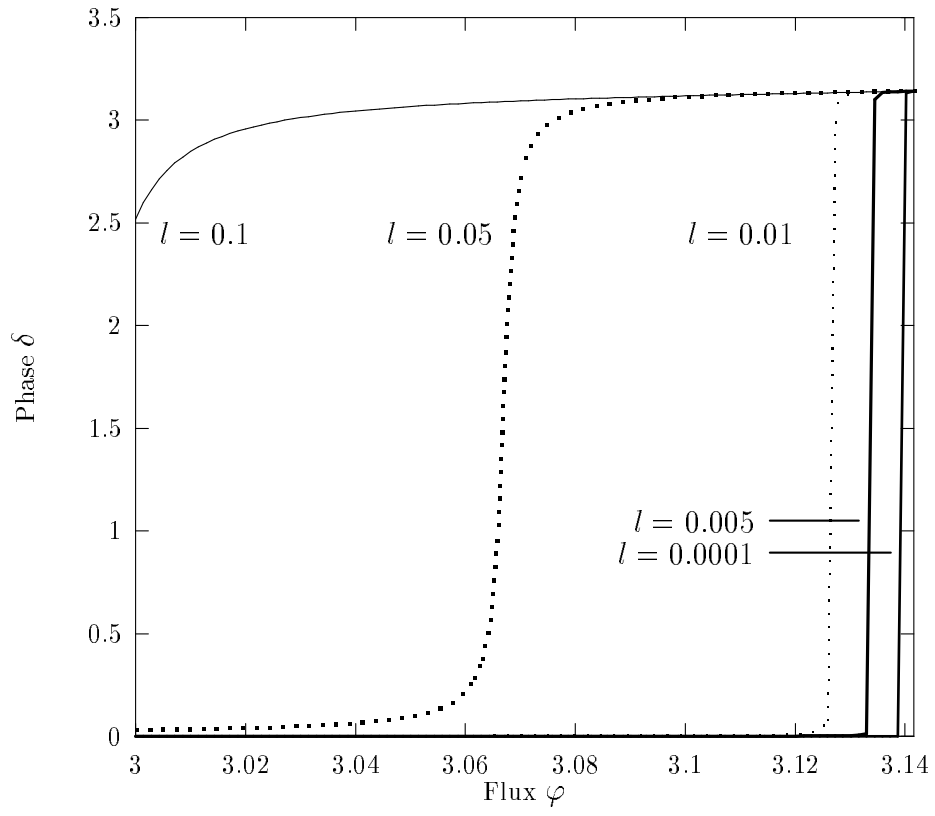


Fig. 6

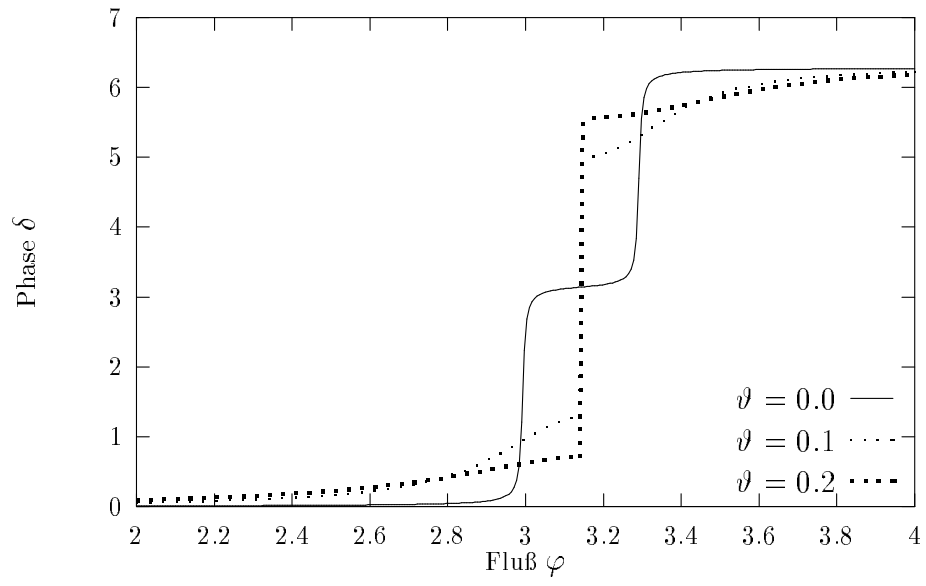


Fig. 7a

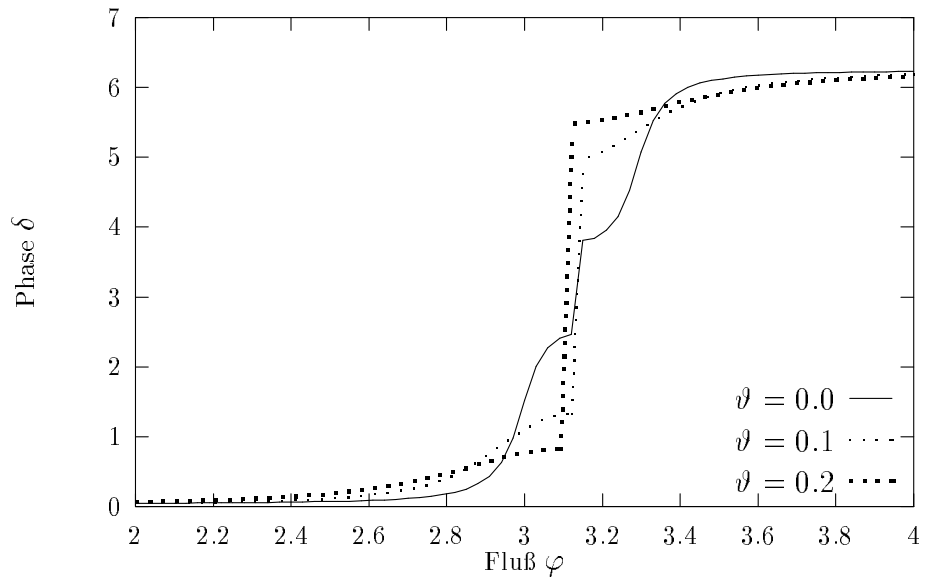


Fig. 7b

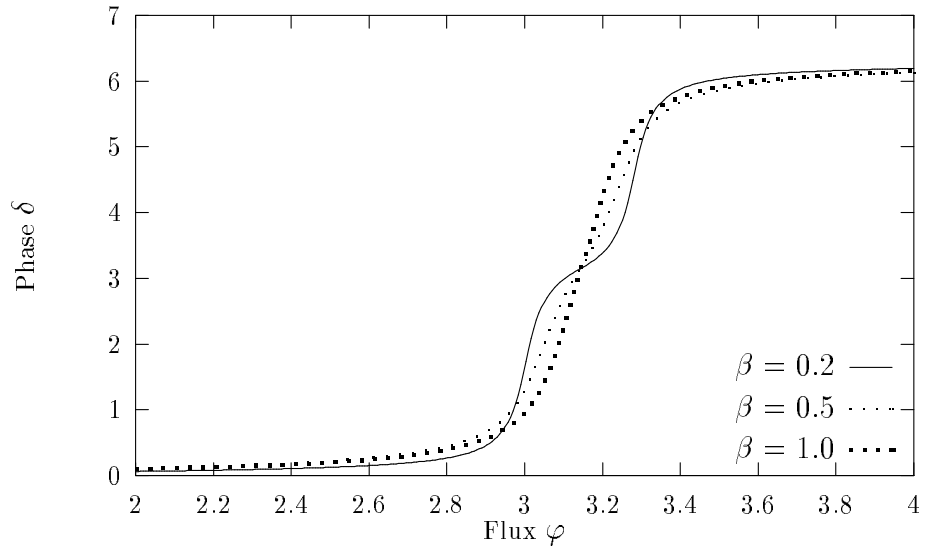


Fig. 8a

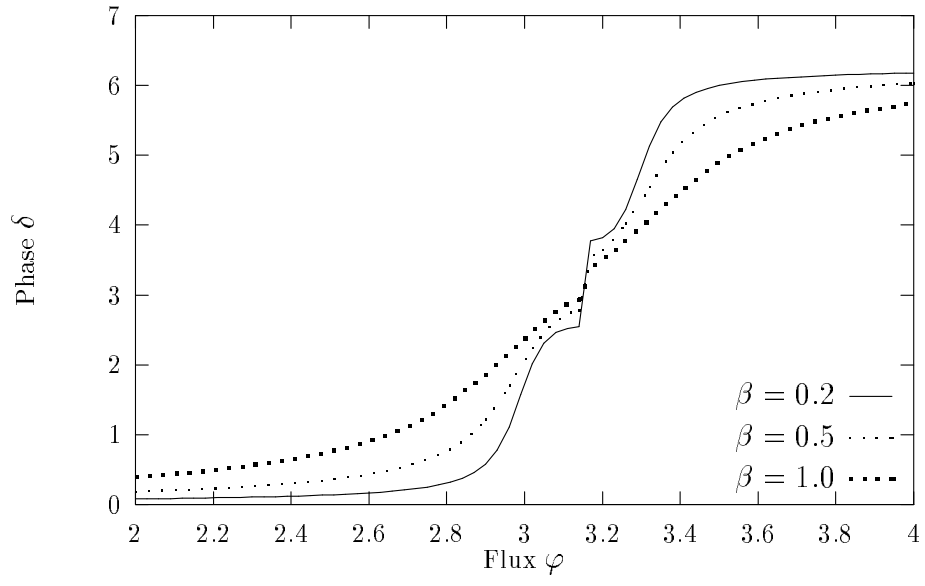


Fig. 8b

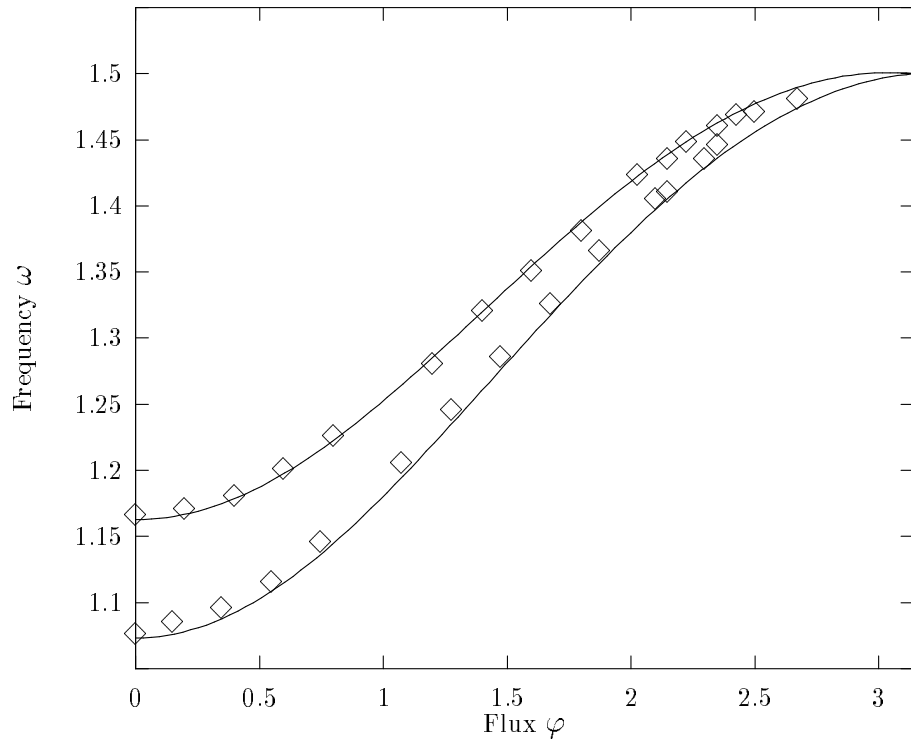


Fig. 9a

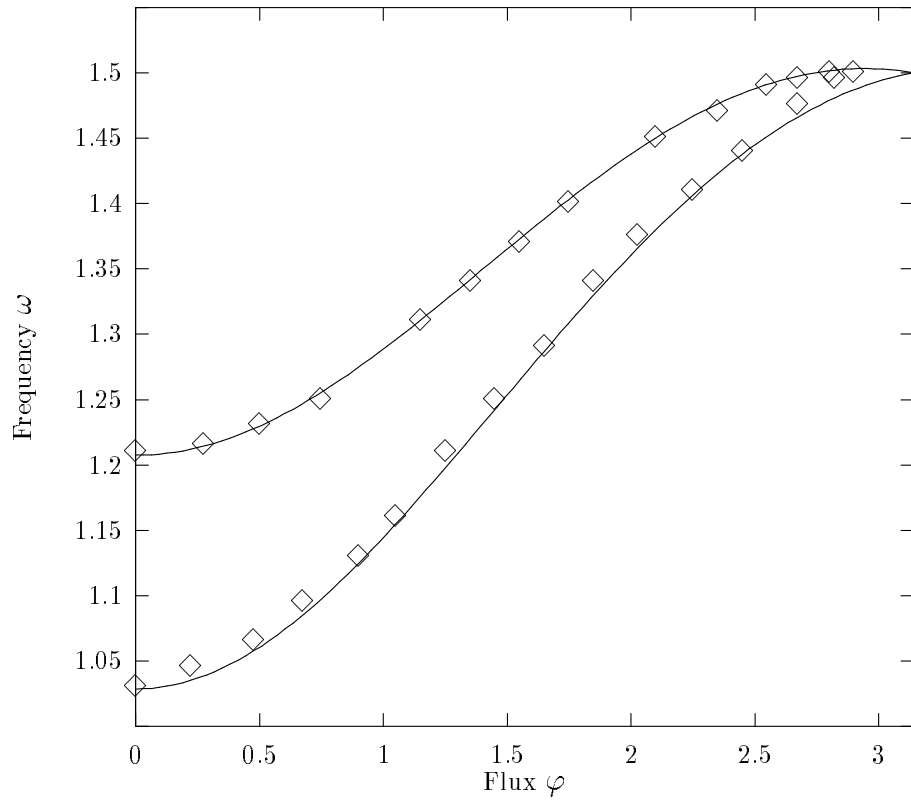


Fig. 9b

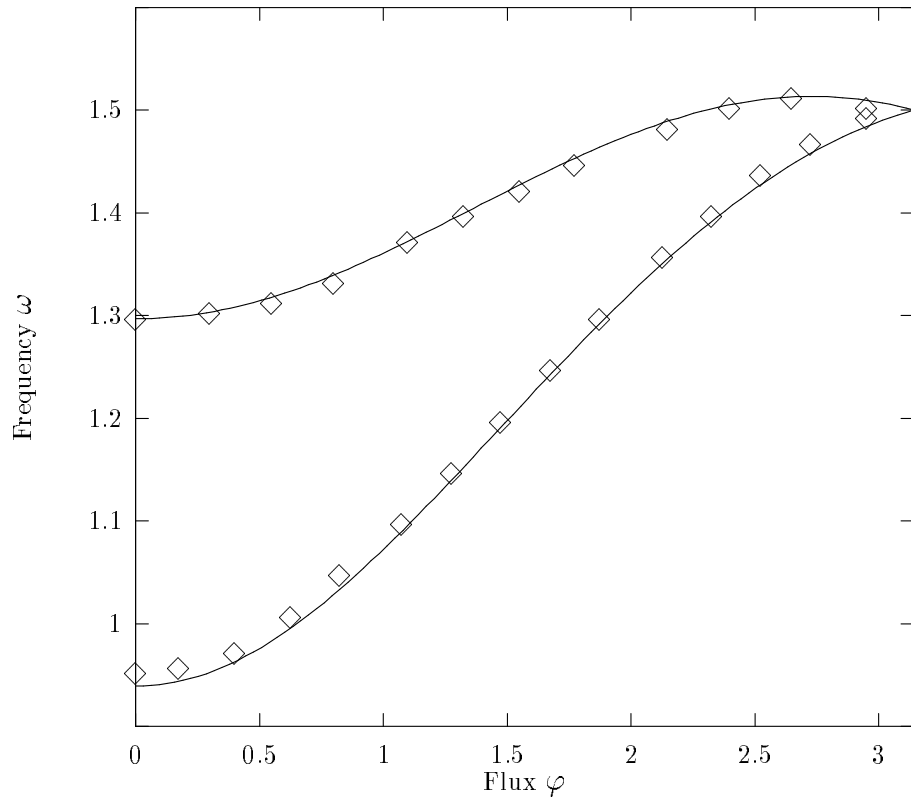


Fig. 9c